Electronic Supplementary Information

A quinoxaline–diaminomaleonitrile conjugate system for colorimetric detection of Cu^{2+} in 100% aqueous medium: observation of aldehyde to acid transformation

Riya Bag,[a] Yeasin Sikdar,[a] Sutapa Sahu,[a] Pinaki Saha,[a] Jayanta Bag,[a] Kuntal Pal*[a] and Sanchita Goswami*[a]

[a] Department of Chemistry, University of Calcutta, 92, A.P.C. Road, Kolkata, India.

E–mail: sgchem@caluniv.ac.in (SG), kpchem@caluniv.ac.in (KP)

Contents of the Supporting Information

Page No.

Fig. S1 ^{1}H NMR spectrum of **H_2qm** in d_6–DMSO. S3

Fig. S2 ^{13}C NMR spectrum of **H_2qm** in d_6–DMSO. S4

Fig. S3 ESI–MS Spectrum of **H_2qm**. S5

Fig. S4 ESI–MS Spectrum of **[$(Hqm)_2Cu$]** complex. S6

Fig. S5 FTIR Spectrum of (A) **H_2qm**, **[$(Hqm)_2Cu$]** and **[$(qa)_2Cu(H_2O)_2$]** complex and (B) **H_2qlm**, **[$(Hqlm)_2Cu$]** and **[$(qla)_2Cu(H_2O)_2$]** complex. S7

Fig. S6 (A) The stability of **H_2qm** in water on changing the pH. (B) Absorbance of **H_2qm** (10 μM) in absence and in presence of Cu^{2+} at different pH values in aqueous solution. S7

Fig. S7 Plot of absorbance *vs* concentration of Cu^{2+} at 562 nm to calculate limit of detection (LOD). S8

Fig. S8 Anion independent absorbance behavior of **H_2qm** in presence of various Cu^{2+} salts [e.g. $CuCl_2$, $CuBr_2$, $Cu(NO_3)_2$, $Cu(ClO_4)_2$, $CuSO_4$ and $Cu(OAC)_2$] in HEPES–buffer solution (25 mM, pH = 7.4). S8

Fig. S9 Job's plot for the determination of **H_2qm–Cu^{2+}** (2:1) complex stoichiometry using absorbance values. S9

Fig. S10 Benesi−Hildebrand plot for the determination of binding constant between **H_2qm** and Cu^{2+}. S9

Fig. S11 Absorption Spectra of H_2qm in presence of Cu^{2+} ion with sequential addition of EDTA. S10

Fig. S12 B3LYP gas phase optimized molecular geometry along with bond distances label for (A) **[(Hqm)$_2$Cu]** and (B) **H_2qm**. S10

Fig. S13 SCF spin density contour plot for complex **[(Hqm)$_2$Cu]** in water. (A) positive spin only; (B) both spin (yellow: positive spin, red: negative spin). S11

Fig. S14 Frontier molecular orbital contour plot for **H_2qm** calculated in water as solvent. S12

Fig. S15 Frontier molecular orbital contour plot for **[(Hqm)$_2$Cu]** calculated in water as solvent. S13

Fig. S16 Molecular structures of Compound $[(qa)_2Cu(H_2O)_2]$(**2**) in ball and stick representation. C = green; N = blue; O = red, H= black, Cu = navy blue. Symmetry operator for equivalent atom generation: #1 (1–x,1–y,1–z). S14

Fig. S17 UV–Vis absorption spectrum of (A) **H_2qm**, **[(Hqm)$_2$Cu]** and **[(qa)$_2$Cu(H$_2$O)$_2$]** complex and (B) **H_2qlm**, **[(Hqlm)$_2$Cu]** and **[(qla)$_2$Cu(H$_2$O)$_2$]** complex in DMSO medium. S15

Fig. S18 UV–Vis absorbance of **H_2qm** as a function of Cu^{2+} concentration at 562 nm. S15

Table S1 Colorimetric chemosensors for naked–eye detection of Cu^{2+} found in literature. S16

Table S2 Percentage contributions of atomic orbitals to selected molecular orbitals (MO) which are involved in vertical transition for **H_2qm** and **[(Hqm)$_2$Cu]** and calculated in water as solvent. S19

Table S3 low–energy excitation wavelengths (λ) and oscillator strengths (OS) for **H_2qm** and **[(Hqm)$_2$Cu]** in water. S20

Table S4 XYZ coordinate of gas phase optimized molecular geometry for **[(Hqm)$_2$Cu]** and **H_2qm.** S21

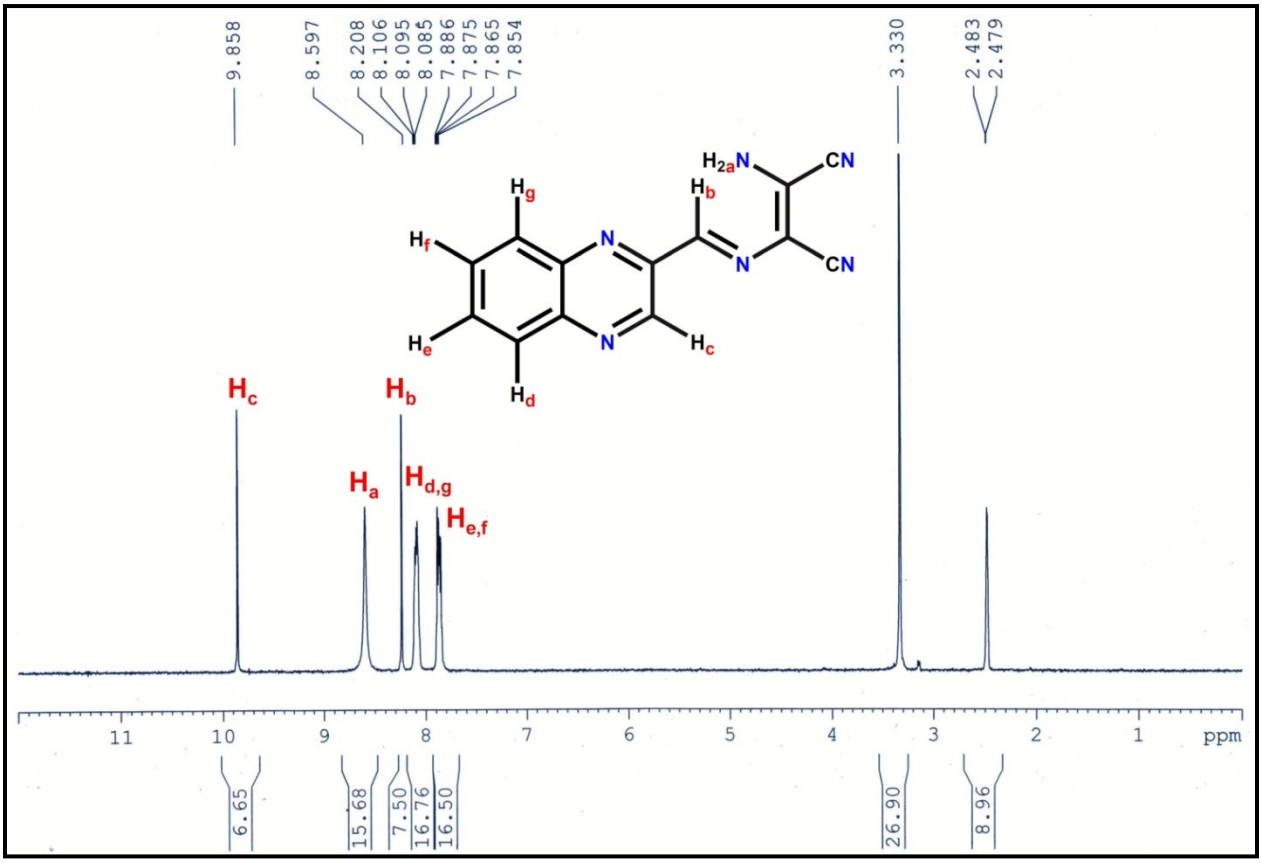

Fig. S1 ^{1}H NMR spectrum of **H_2qm** in d_6–DMSO.

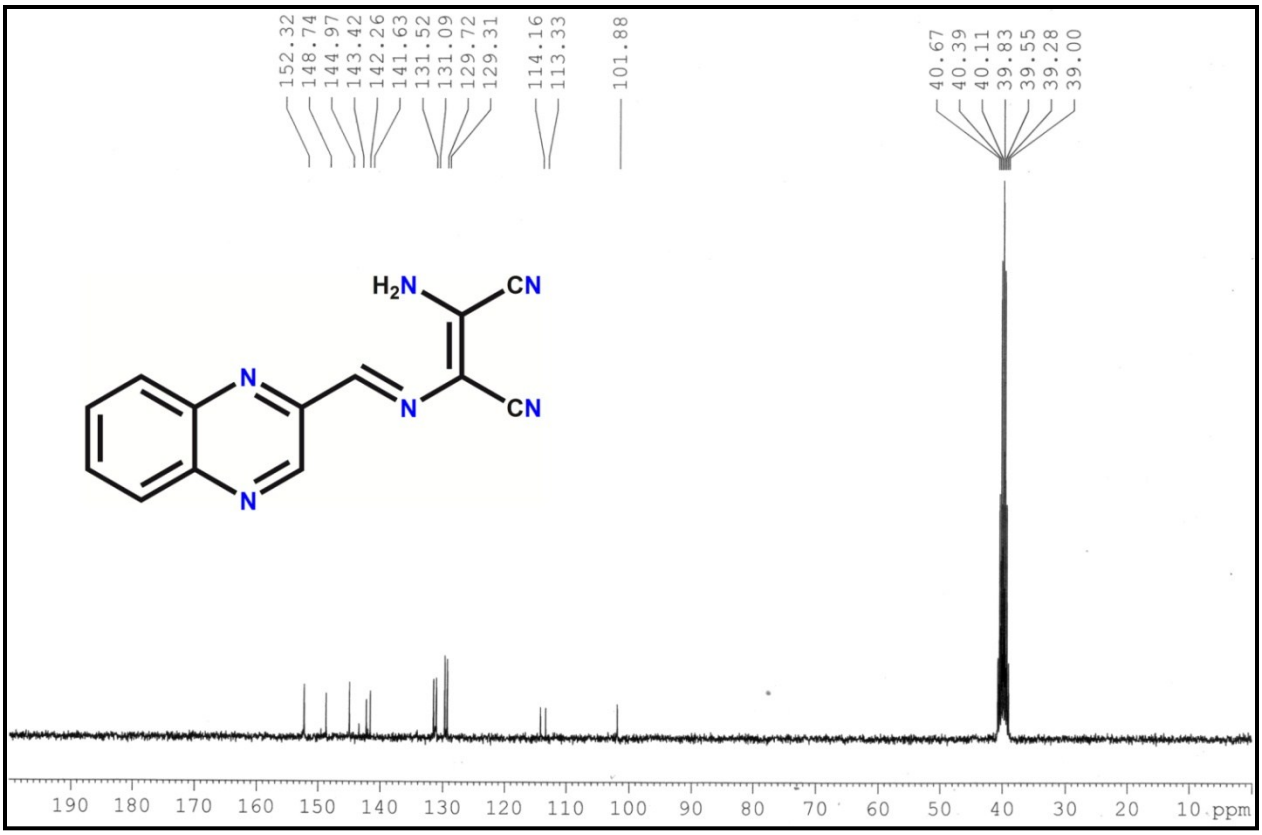

Fig. S2 ^{13}C NMR spectrum of **H_2qm** in d_6–DMSO.

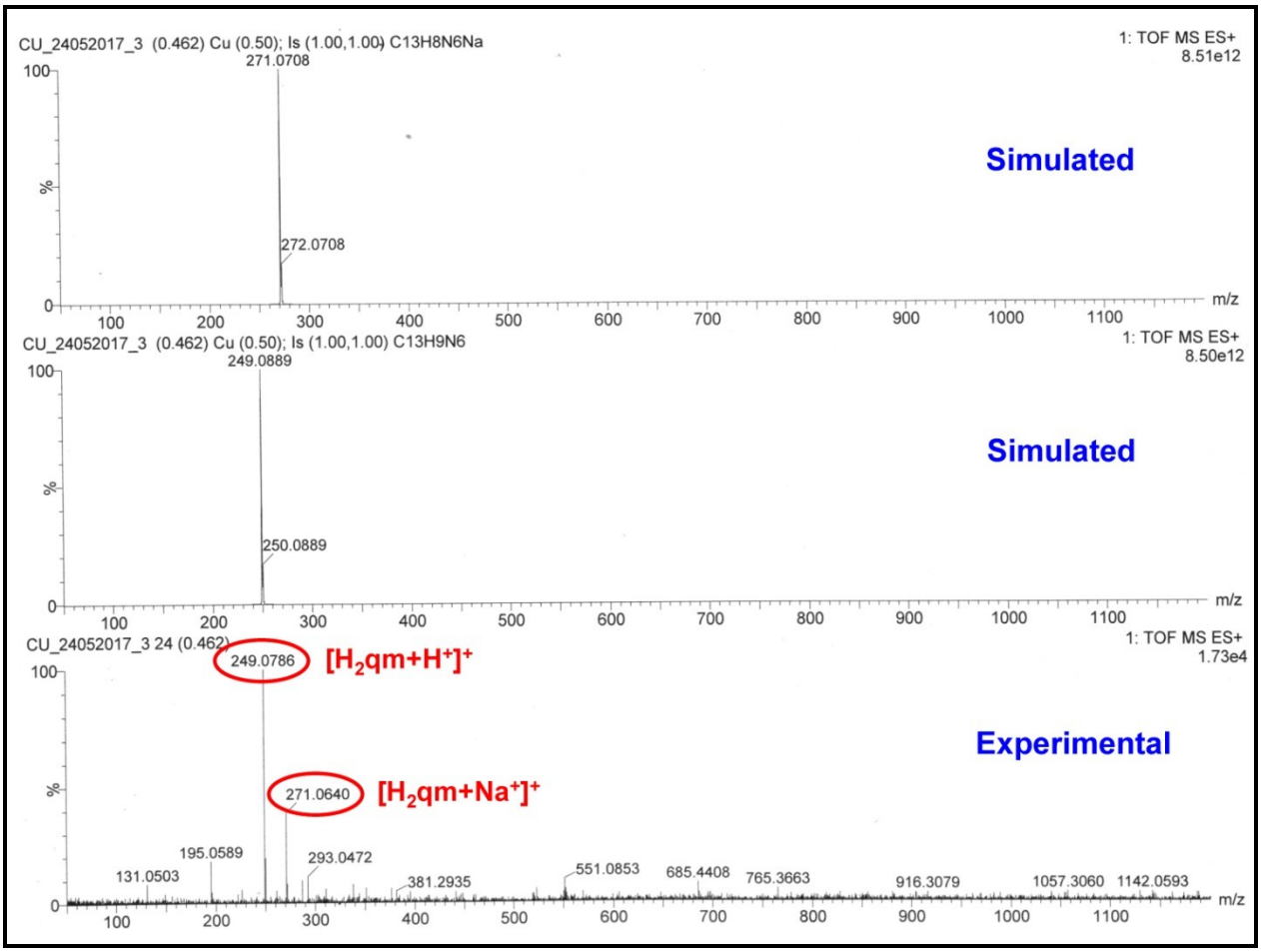

Fig. S3 ESI–MS Spectrum of **H_2qm**.

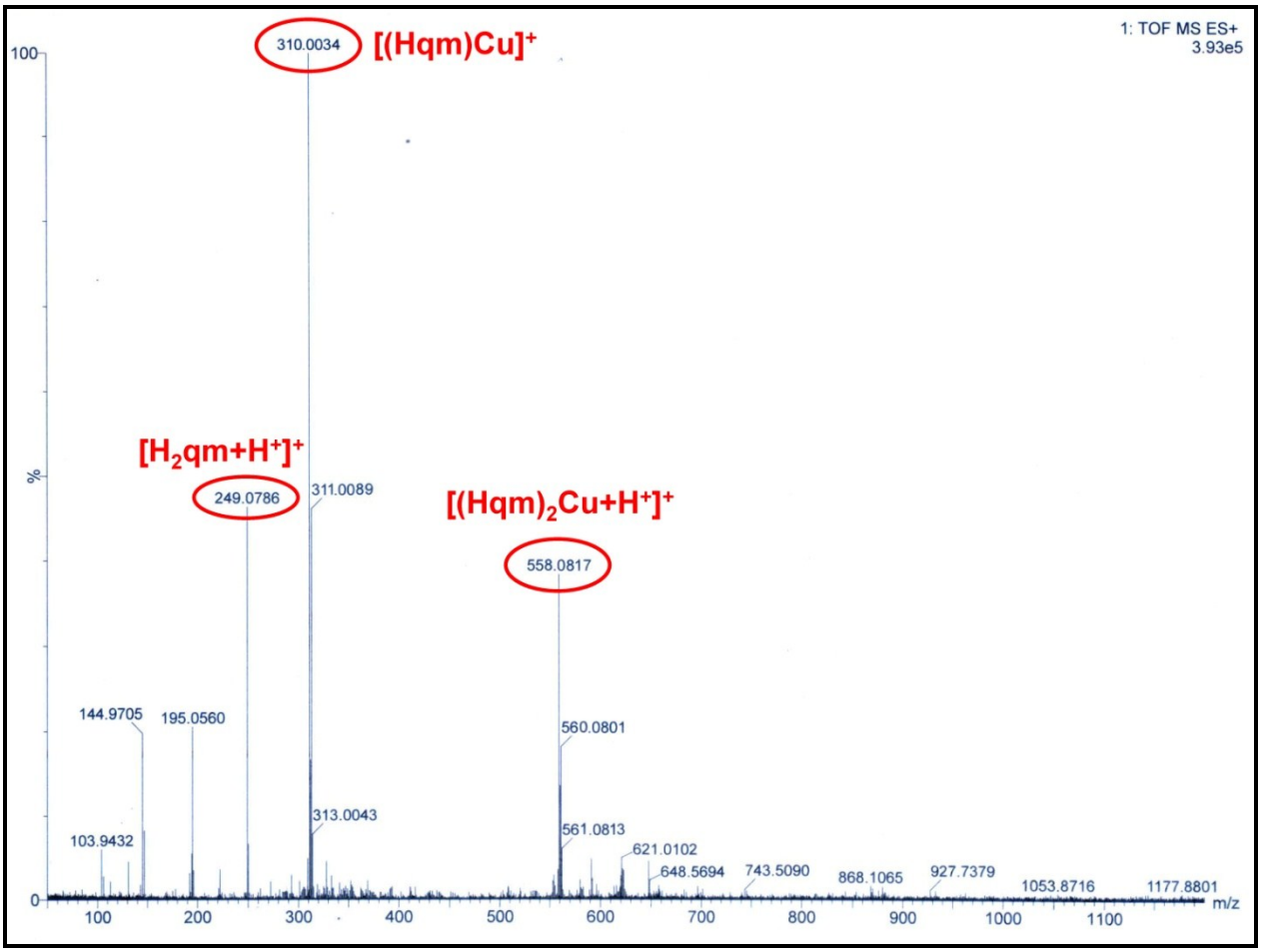

Fig. S4 ESI–MS Spectrum of **[(Hqm)$_2$Cu]** complex.

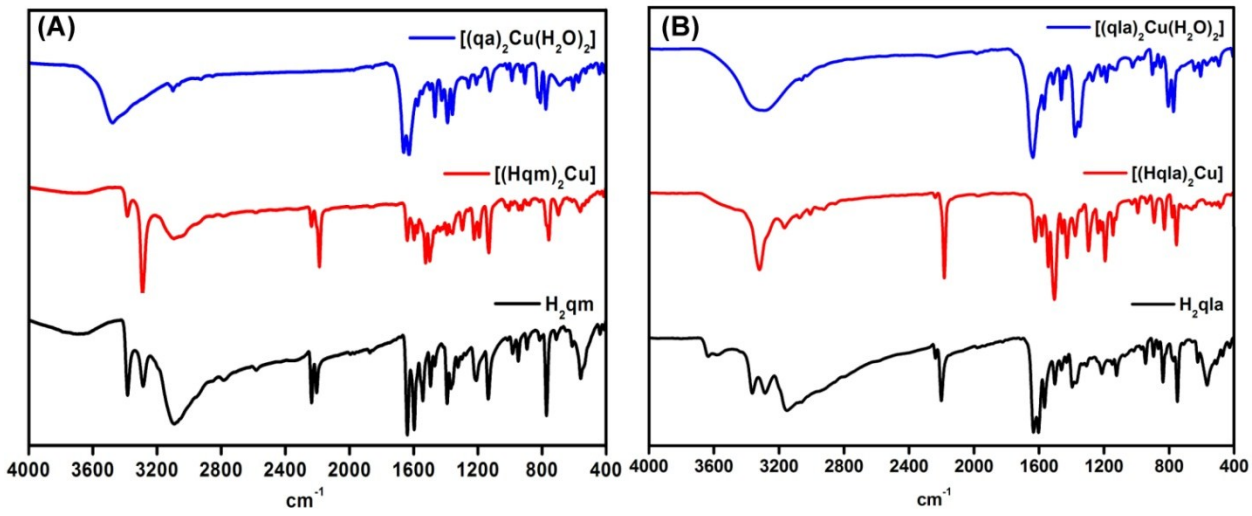

Fig. S5 FTIR Spectrum of (A) **H_2qm**, **[(Hqm)$_2$Cu]** and **[(qa)$_2$Cu(H_2O)$_2$]** complex and (B) **H_2qlm**, **[(Hqlm)$_2$Cu]** and **[(qla)$_2$Cu(H_2O)$_2$]** complex.

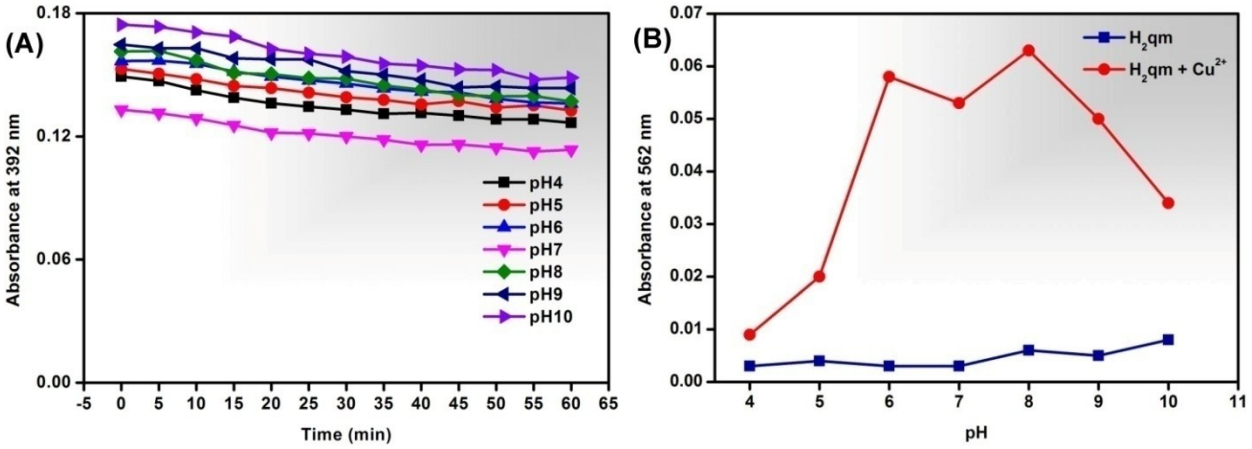

Fig. S6 (A) The stability of **H_2qm** in water on changing the pH. (B) Absorbance of **H_2qm** (10 μM) in absence and in presence of Cu^{2+} at different pH values in aqueous solution.

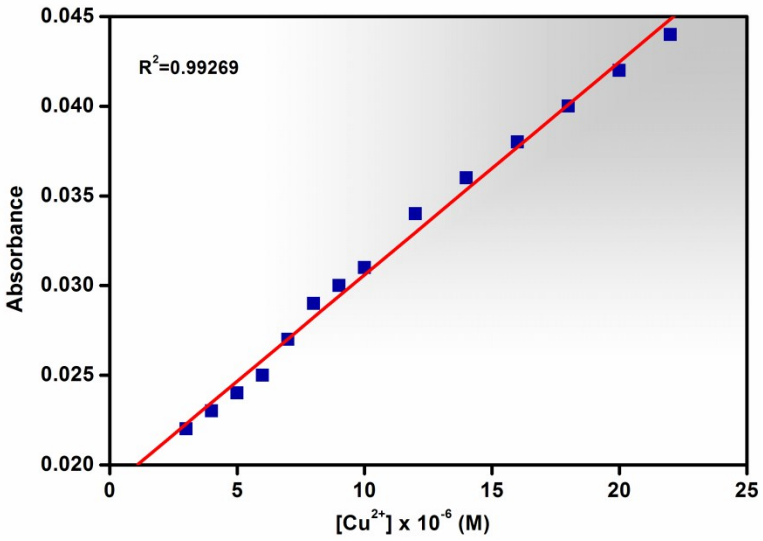

Fig. S7 Plot of absorbance *vs* concentration of Cu^{2+} at 562 nm to calculate limit of detection (LOD).

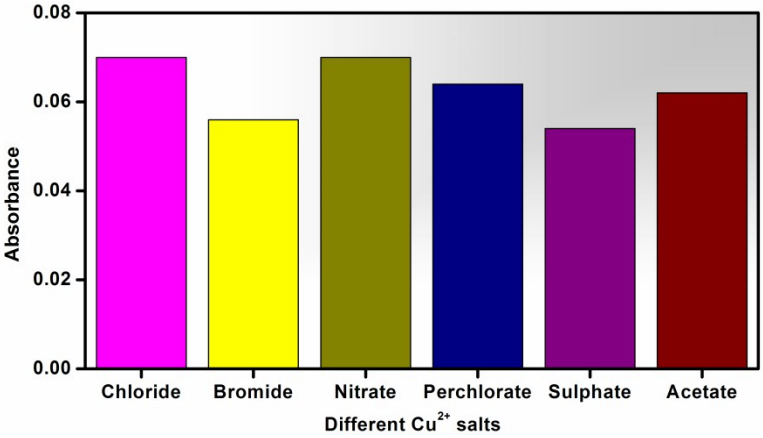

Fig. S8 Anion independent absorbance behavior of **H_2qm** in presence of various Cu^{2+} salts [e.g. $CuCl_2$, $CuBr_2$, $Cu(NO_3)_2$, $Cu(ClO_4)_2$, $CuSO_4$ and $Cu(OAc)_2$] in HEPES–buffer solution (25 mM, pH = 7.4).

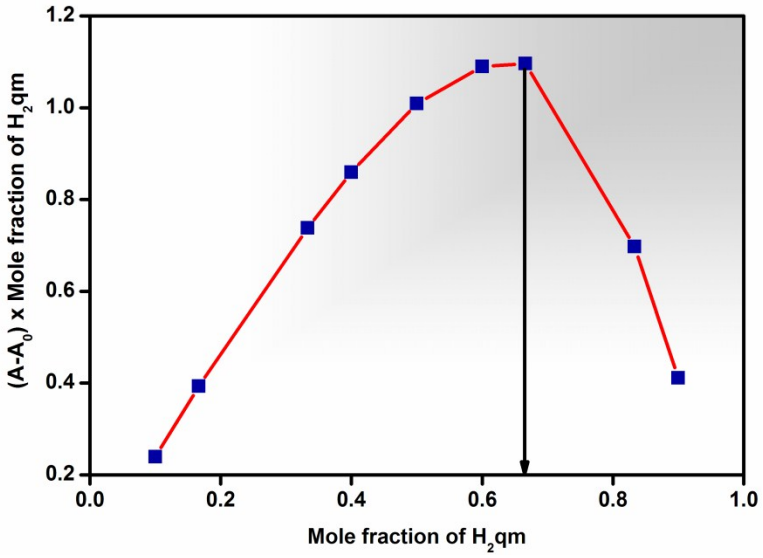

Fig. S9 Job's plot for the determination of **H_2qm–Cu^{2+}** (2:1) complex stoichiometry using absorbance values.

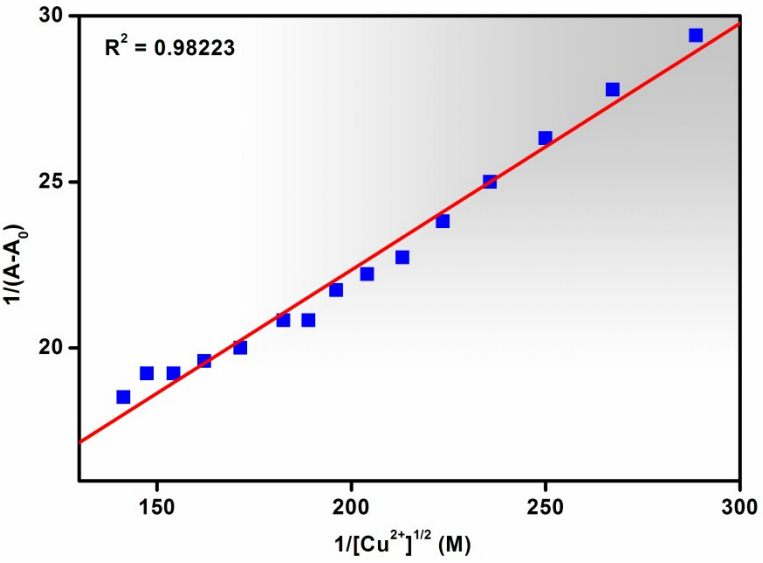

Fig. S10 Benesi−Hildebrand plot for the determination of binding constant between **H_2qm** and Cu^{2+}.

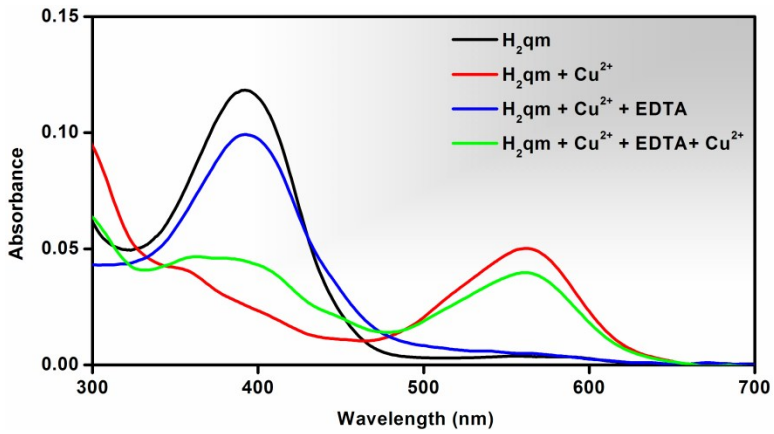

Fig. S11 Absorption Spectra of **H_2qm** in presence of Cu^{2+} ion with sequential addition of EDTA.

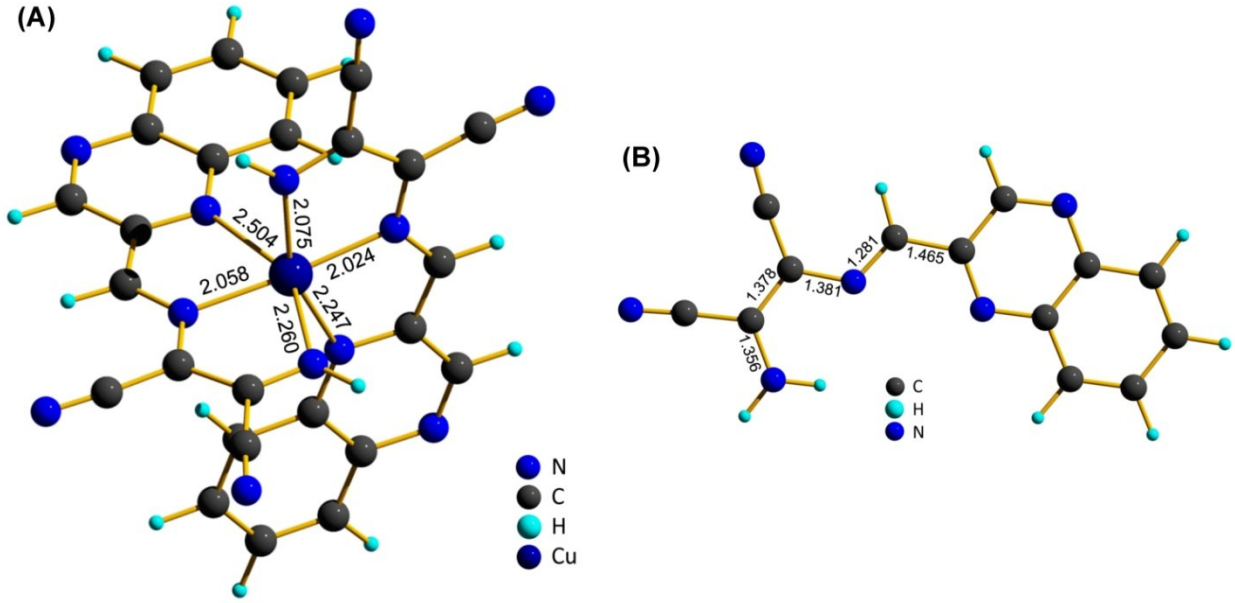

Fig. S12 B3LYP gas phase optimized molecular geometry along with bond distances label for (A) **[$(Hqm)_2$Cu]** and (B) **H_2qm**.

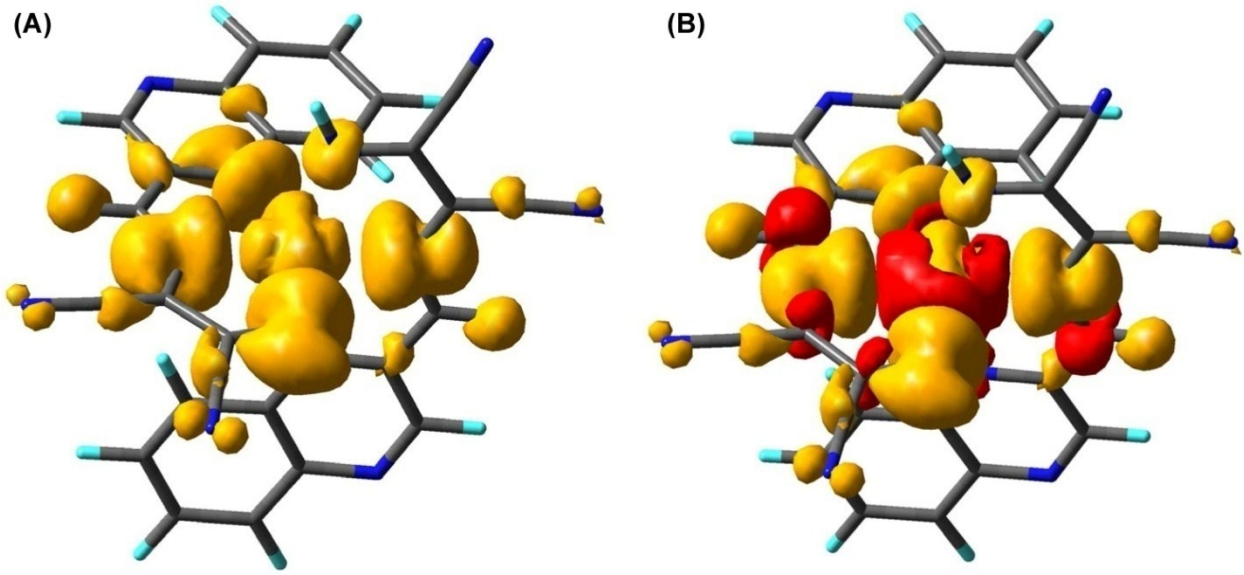

Fig. S13 SCF spin density contour plot for complex **[(Hqm)$_2$Cu]** in water. (A) positive spin only; (B) both spin (yellow: positive spin, red: negative spin).

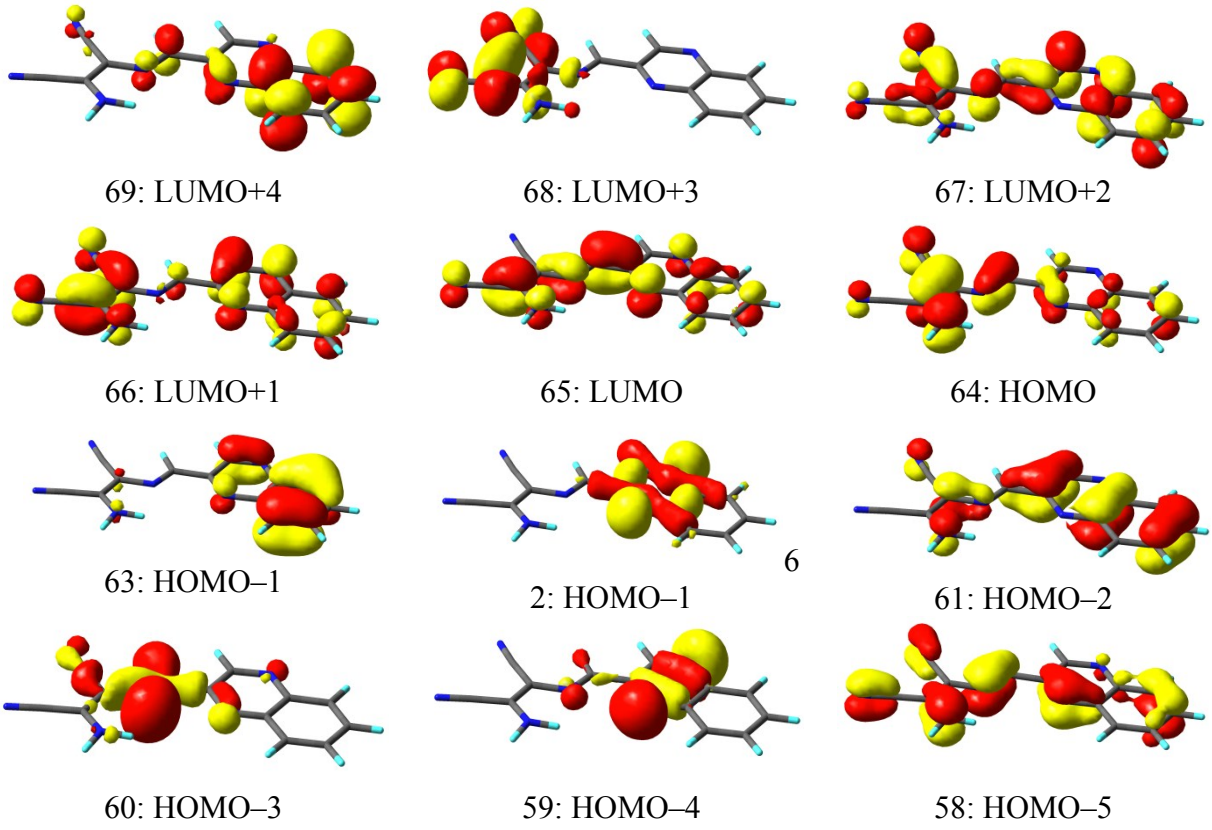

Fig. S14 Frontier molecular orbital contour plot for **H_2qm** calculated in water as solvent.

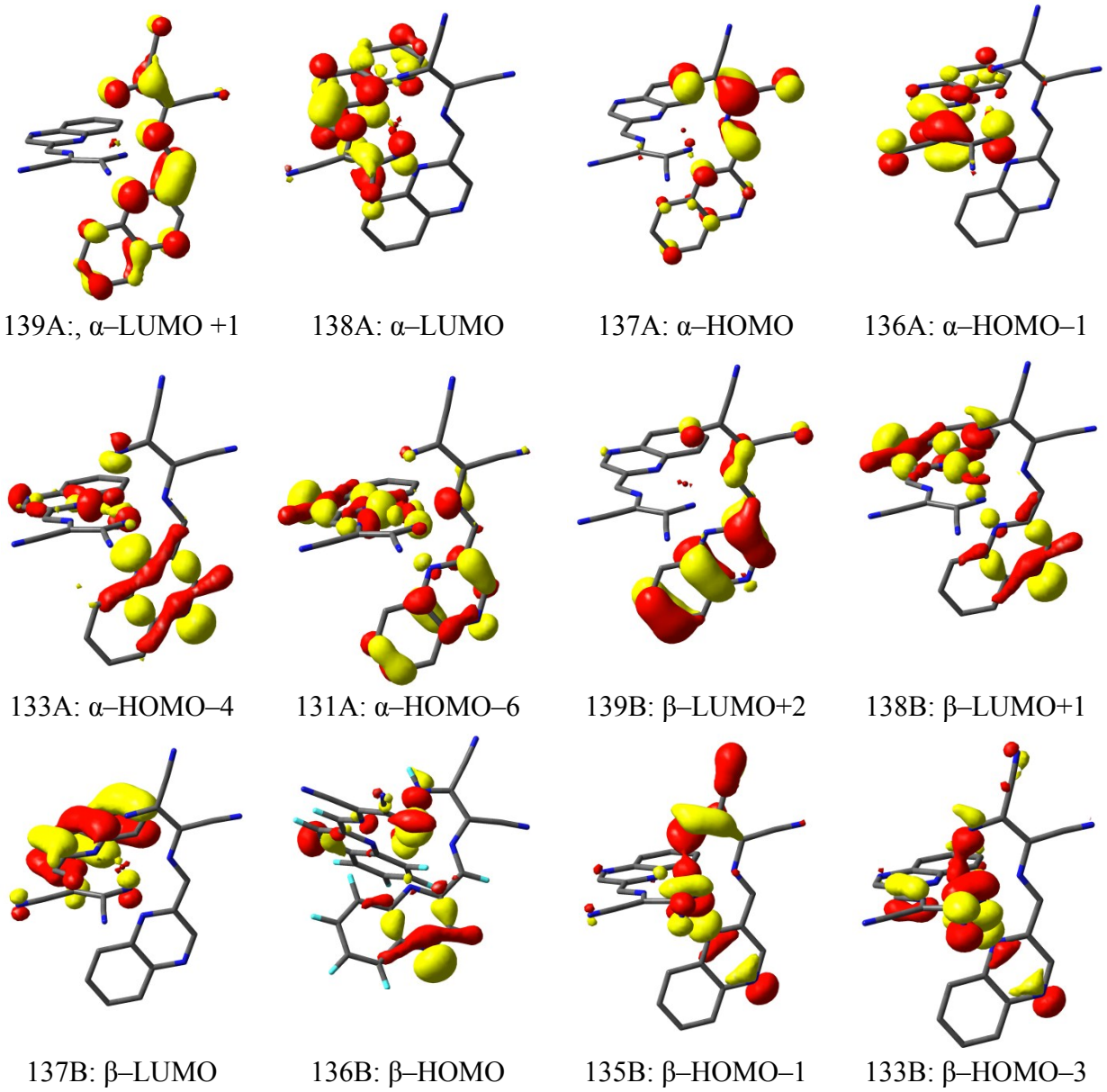

Fig. S15 Frontier molecular orbital contour plot for **[(Hqm)$_2$Cu]** calculated in water as solvent.

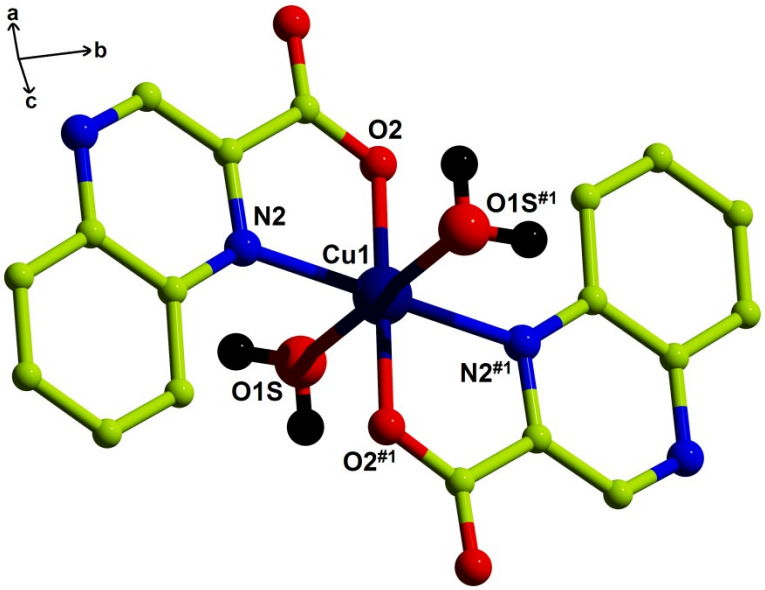

Fig. S16 Molecular structure of compound $[(qa)_2Cu(H_2O)_2]$(**2**) in ball and stick representation. C = green; N = blue; O = red, H= black, Cu = navy blue. Symmetry operator for equivalent atom generation: #1 (1–x,1–y,1–z).

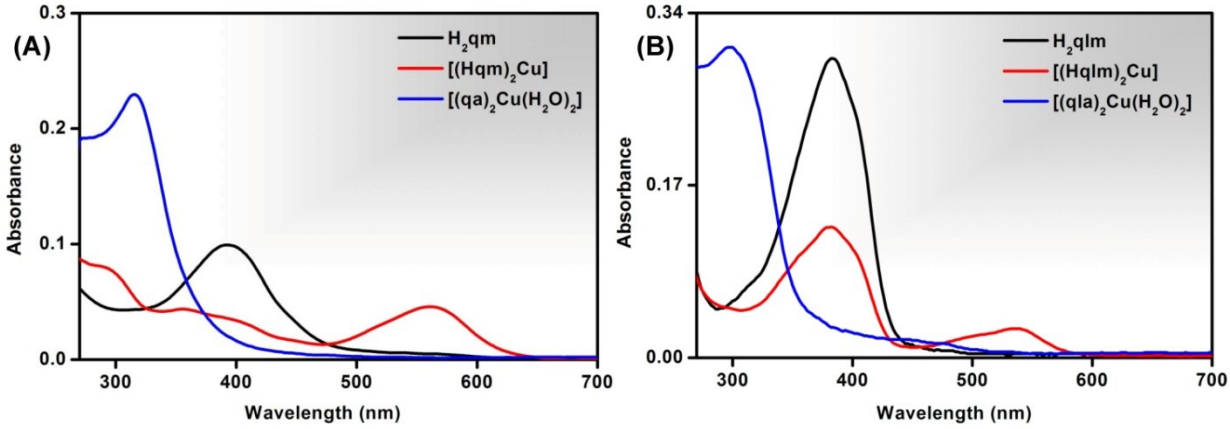

Fig. S17 UV–Vis absorption spectrum of (A) **H_2qm, $[(Hqm)_2Cu]$ and $[(qa)_2Cu(H_2O)_2]$ complex and (B) H_2qlm, $[(Hqlm)_2Cu]$ and $[(qla)_2Cu(H_2O)_2]$** complex in DMSO medium.

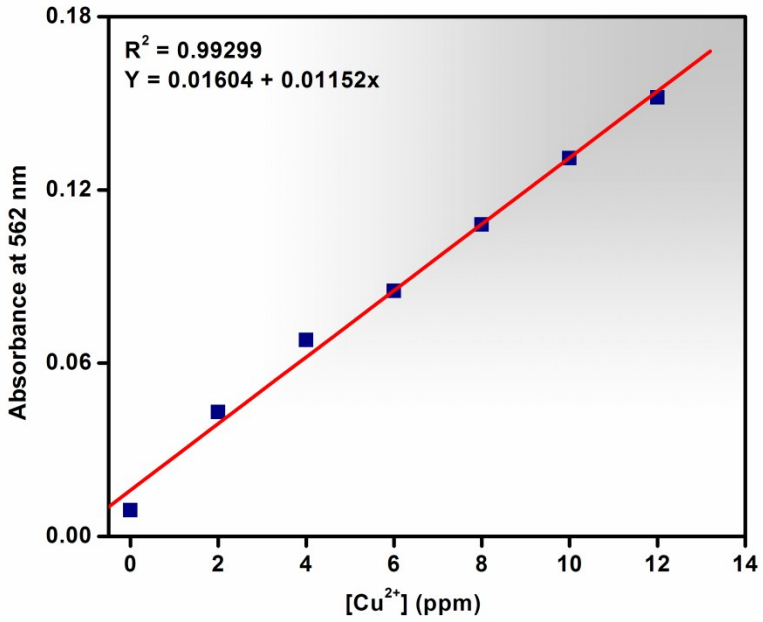

Fig. S18 UV–Vis absorbance of **H_2qm** as a function of Cu^{2+} concentration at 562 nm.

Table S1 Colorimetric chemosensors for naked–eye detection of Cu^{2+} found in literature.

Probe	Water content	Limit of detection	Spectral range	Reference
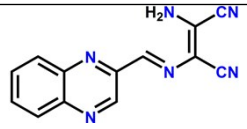	100%	1.64 μM	392 nm to 562 nm	In this work
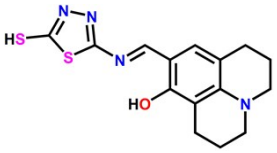	100%	0.9 μM	450 nm to 525 nm	*Dalton Trans.*, 2015, **44**, 9120–9129
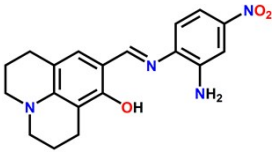	83.3%	0.37 μM	410 nm to 525 nm	*RSC Adv.*, 2015, **5**, 31179–31188
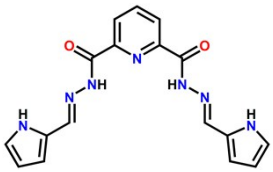	70%	0.004 μM	330 nm to 392 nm	*RSC Adv.*, 2016, **6**, 28194–28199
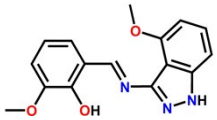	70%	0.14 μM	360 nm to 427 nm	*Tetrahedron*, 2017, **73**, 4750–4757
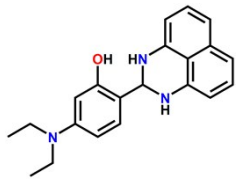	50%	0.0037 μM	320 nm to 408 nm	*ACS Omega,* 2018, **3**, 10471−10480
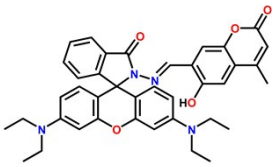	50%	0.028 μM	–	*RSC Adv.*, 2015, **5**, 77965–77972
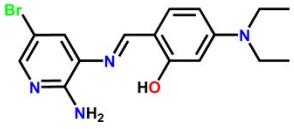	50%	0.0686 μM	404 nm to 478 nm	*Inorganica Chim. Acta,* 2018, **471**, 709–717

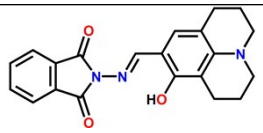	50%	0.14 μM	383 nm to 422 nm	*Ind. Eng. Chem. Res.*, 2017, **56**, 8399–8407
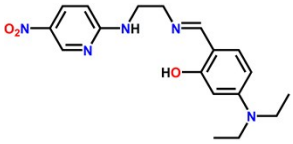	50%	0.88 μM	385 nm to 436 nm	*Inorg. Chem. Commun.*, 2016, **74**, 62–65
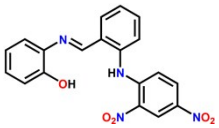	50%	8.77 μM	348 nm to 412 nm	*RSC Adv.*, 2016, **6**, 16586–16597
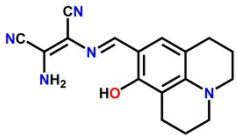	40%	2.1 μM	450 nm to 375 nm	*New J. Chem.*, 2015, **39**, 2580–2587
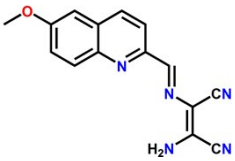	33.3%	0.53 μM	390 nm to 537 nm	*Tetrahedron,* 2017, **73**, 5715–5719
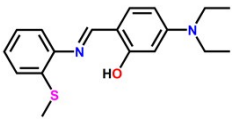	30%	3.89 μM	392 nm to 416 nm	*RSC Adv.*, 2016, **6**, 74400–74408
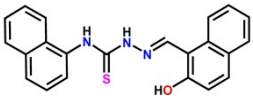	30%	4.64 μM	405 nm to 456 nm	*Dalton Trans.*, 2015, **44**, 18902–18910
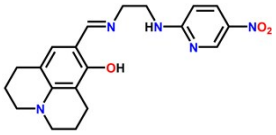	30%	23.5 μM	382 nm to 450 nm	*RSC Adv.*, 2015, **5**, 86463–86472
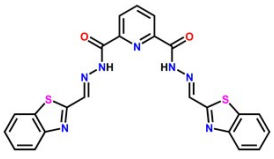	20%	0.12 μM	332 nm to 362 nm	*New J. Chem.*, 2018, **42**, 8567–8576
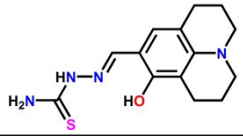	20%	0.48 μM	382 nm to 416 nm	*Tetrahedron,* 2016, **72**, 875–881

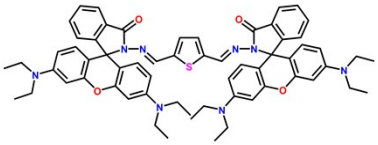	20%	1.01 μM	–	*Photochem. Photobiol. Sci.*, 2017, **16**, 1441–1448
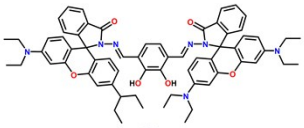 Rh1 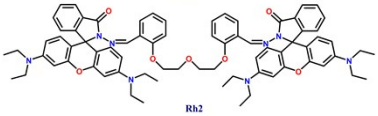 Rh2	10%	Rh1: 0.0122 μM Rh2: 0.79 μM	–	*RSC Adv.*, 2016, **6**, 106631–106640
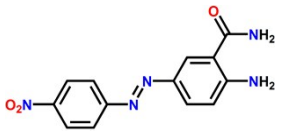	10%	2.39 μM	368 nm to 293 nm	*J. Photochem. Photobiol., A*, 2018, **367**, 22–31
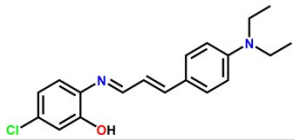	9%	0.12 μM	407 nm to 530 nm	*Sens. Actuators B*, 2016, **225**, 221–227

Table S2 Percentage contributions of atomic orbitals to selected molecular orbitals (MO) which are involved in vertical transition for **H_2qm** and **[(Hqm)$_2$Cu]** and calculated in water as solvent.

[(Hqm)$_2$Cu]		**H_2qm**	
Molecular Orbital	**Major contribution**	**Molecular Orbital**	**Major contribution**
139A: α–LUMO +1	π* of (π of quinoxaline–imine C–H) and (π malenonitrile–imine N)	69: LUMO+4	π* of quinoxaline
138A: α–LUMO	π* of (π of quinoxaline–imine C–H) and (π malenonitrile–imine N)	68: LUMO+3	π* of C≡N group
137A: α–HOMO	π* of malenonitrile N and (π* malenonitrile–imine C–H)	67: LUMO+2	π* of quinoxaline
136A: α–HOMO–1	π* of malenonitrile N and (π* malenonitrile–imine C–H)	66: LUMO+1	π of C–CN bond
133A: α–HOMO–4	p_x of quinoxaline N	65: LUMO	π* of CNC–CCN bond and π of N=CH imine
131A: α–HOMO–6	π C=C in quinoxaline	64: HOMO	π of CNC–CCN bond and π of N=CH imine
139B, β–LUMO+2	π C=C in quinoxaline	63: HOMO–1	π of quinoxaline
138B: β–LUMO+1	p_x of quinoxaline N	62: HOMO–2	π* of (p_x of N atoms of Ph–N bonds) and p_x of N–Ph–N quinoxaline carbon) atoms
137B: β–LUMO	π C=C in quinoxaline	61: HOMO–3	π of quinoxaline
136B: β–HOMO	p_x of quinoxaline N	60: HOMO–4	P_y of N atoms of N=CH imine group
135B: β–HOMO–1	p_x of quinoxaline N and π of malenonitrile	59: HOMO–5	Non–bonding p_x of N atoms of Ph–N bonds
133B: β–HOMO–3	p_x of quinoxaline N and π of malenonitrile	58: HOMO–6	π of C–CN bond and N=CH imine

Table S3 low–energy excitation wavelengths (λ) and oscillator strengths (OS) for **H_2qm** and **[(Hqm)$_2$Cu]** in water.

States	Major contribution, (%)	λ (nm), (f)	Transition type	λ_{max} (nm)	λ_{max} (nm, experimental) in Water
		[(Hqm)$_2$Cu]			
11	136A –> 139A, (17) 137A –> 139A, (17) 135B –> 139B, (41) 136B –> 139B, (22)	536 (0.0998)	ILCT (π–π*)		
13	136A –> 138A, (42) 135B –> 138B, (41)	526.39 (0.3782)	ILCT (π–π*)	518	562
14	136A –> 139A, (22) 137A –> 139A, (27) 135B –> 139B, (19) 136B –> 139B, (28)	506.40 (0.4247)	ILCT (π–π*)		
24	131A –> 138A, (12) 133A –> 138A, (23) 133B –> 138B, (37)	405 (0.335)	ILCT (π–π*)	404	392
		H_2qm			
1	64 –> 65, (98)	421 (0.7378)	ILCT (π –π*)	421	392
4	61 –> 65, (24) 64 –> 66, (69)	320 (0.2825)	ILCT (π –π*)	319	314
9	64 –> 67, (52)	264 (0.3352)			
10	64 –> 68, (79)	261 (0.0676)			
12	61 –> 66, (72) 63 –> 67, (19)	252.86 (0.0261)			

*ILCT = Intra–ligand charge transfer

Table S4 XYZ coordinate of gas phase optimized molecular geometry for **[(Hqm)$_2$Cu]** and **H$_2$qm**.

[(Hqm)$_2$Cu]

N	–1.13310	–0.78850	1.31230
C	–2.26500	–1.52830	1.20470
C	–0.52100	–0.76790	2.48960
N	0.86490	–0.79050	–1.43520
C	0.24620	–0.68070	–2.61130
C	1.81710	–1.75220	–1.30690
N	1.16940	0.71700	1.67600
C	2.31070	1.46420	1.73860
C	0.68310	0.01310	2.65840
N	–1.00210	1.11360	–1.75270
C	–1.91030	2.12440	–1.66760
C	–0.76040	0.34120	–2.76790
C	–1.93600	2.77720	–0.40670
C	–2.74460	2.45050	–2.76090
N	–1.12800	2.37970	0.54060
H	–1.18160	2.89380	1.40840
N	–3.38630	2.64230	–3.70370
N	1.96900	2.09280	–0.52840
C	2.68970	2.16240	0.55320
H	2.34230	2.63570	–1.29650
C	–2.85440	3.86750	–0.18660
N	–3.57160	4.73990	0.03690
C	3.90420	2.94960	0.58440
H	–1.29150	0.44980	–3.70770
C	0.56750	–1.55200	–3.69090
C	2.11770	–2.61490	–2.40900
N	1.46880	–2.48980	–3.59880
C	3.10510	–3.61270	–2.26640
C	2.52660	–1.92160	–0.09610
C	3.06720	1.50750	2.93280
N	3.62060	1.47560	3.94860
C	–2.76150	–2.26700	2.32300
C	–2.97490	–1.58000	–0.01850
C	–1.03370	–1.51170	3.59630
N	4.86080	3.58920	0.54230
N	–2.11290	–2.23920	3.52180
C	–3.93780	–3.03360	2.18730
H	–0.51330	–1.48040	4.54760
H	0.04790	–1.44160	–4.63620
H	1.18110	–0.00240	3.62270
C	–4.11740	–2.33260	–0.11930
H	–2.60250	–1.01200	–0.85750
H	–4.65820	–2.36410	–1.05510
C	–4.60280	–3.06590	0.98700
H	–5.50550	–3.65120	0.88300
H	–4.28850	–3.58140	3.05020
C	3.48300	–2.89930	0.00930
H	2.30760	–1.26870	0.73240
C	3.77590	–3.75240	–1.07830
H	4.02420	–3.01770	0.93760
H	3.30760	–4.24690	–3.11730
H	4.53420	–4.51460	–0.96900
Cu	0.12810	0.85510	–0.09420

H_2qm

C	–4.57828312	–1.86783372	0.03254433	N	–2.84437401	1.91223046	–0.02560706
C	–3.21194546	–1.77305412	0.02897061	C	0.73901038	0.97795642	–0.01692038
C	–2.59055937	–0.49863890	0.00929365	H	1.09251375	2.01145446	–0.02762611
C	–3.40771330	0.67476159	–0.00668573	N	1.55142087	–0.01246878	–0.00868511
C	–4.81444402	0.54376086	–0.00240886	C	2.92133122	0.16184365	–0.00267550
C	–5.38450964	–0.70338472	0.01683588	C	3.68449417	–0.98479687	–0.02293876
H	–5.05229005	–2.83950268	0.04743978	N	3.12848874	–2.21836771	–0.10495162
H	–2.57762135	–2.64788397	0.04058573	H	3.67899522	–3.03416674	0.09010841
H	–5.41047303	1.44512711	–0.01470474	H	2.12366299	–2.26556631	–0.02675092
H	–6.46095491	–0.80461962	0.02004858	C	5.11383768	–0.92349700	0.01308555
C	–1.53747890	1.96279785	–0.02837210	C	3.51822689	1.45777026	0.02182584
C	–0.71491640	0.79772813	–0.01236653	N	6.26518742	–0.92677133	0.05086607
H	–1.07783172	2.94541275	–0.04323076	N	3.89276420	2.54982196	0.04391204
N	–1.24181603	–0.41340685	0.00632312				